SCIREA Journal of Mechanics

http://www.scirea.org/journal/Mechanics

September 18, 2023

Volume 4, Issue 1, February 2023

http://dx.doi.org/10.54647/mechanics130034

The Solution Equivalent of the Navier-Stokes Equation in HPLC

Hubert M. Quinn[1]

[1]The Wrangler Group LLC, 40 Nottinghill Road, Brighton, Ma. 02135, United States

Email: hubert@wranglergroup.com; Tel: 857-540-0570

Abstract

The Navier-Stokes equation is generally considered the ultimate mathematical expression for the dictates of the Laws of Nature which pertain to transport phenomena in the field of fluid dynamics. It is written and typically discussed, however, in the form and jargon of advanced mathematics. This makes it very difficult for any nonmathematician to understand, and this, in part, is why it remains unsolved for most applications. The essence of the equation, however, has nothing to do with mathematics and everything to do with the underlying physics surrounding the fluid transport mechanisms involved in any given fluid flow embodiment. Accordingly, it is the non-mathematical "solution equivalent" of the N-S equation that is important to the practitioner of fluid dynamics. In the case of HPLC (High Pressure Liquid Chromatography), for instance, this means the physics underlying fluid flow through conduits packed with partially porous solid particles. Recently, 2019, a new fluid flow model (QFFM) was published which contains, embedded in its framework, the "solution equivalent" for the N-S equation in chromatographic columns. This novel fluid flow model teaches that an empty HPLC column is a special case of the same column packed with solid particles. In fact, one is the mirror image of the other. The difference between the two is defined by the choice of independent variables. Thus, by setting the value of three independent variables in the QFFM, the complexity of the advanced mathematics in the Navier-Stokes equation can be avoided. If one considers "matter" and "anti-matter" to be the mirror image of one another, however, one can easily rationalize the rules of engagement which underlie this phenomenon in the context of the Navier-Stokes equation. In this paper we will explain how the QFFM rationalizes the fundamental issues of the Navier-Stokes equation, providing the

"solution equivalent", in the jargon of classical mechanics, as opposed to that of advanced mathematics, for fluid flow through HPLC columns.

Key Words: Conduit Porosity; Hypothetical Q particles; Particle porosity: Packed beds; Column Permeability.

Highlights

- An empty conduit is a special case of a packed conduit containing particles with a solid skeleton
- The one is the mirror image of the other
- The difference between the two flow embodiments is defined by the choice of independent variables
- Packed conduits and empty conduits are seamlessly accommodated in the QFFM framework
- The QFFM is certifiable over the entire fluid flow regime from creeping flow to fully developed turbulence

1. Introduction

Let us begin at the beginning. Most practitioners will say that the first real attempt to characterize the flow of fluids through closed conduits was made by Poiseuille circa 1846[1], in the case of empty conduits, and by Henry Darcy in 1856 [2], in the case of conduits packed with solid obstacles. The former's work led to what is known today as Poiseuille's Law [3] and the latter's work to what is known as Darcy's Law [4]. Both these Laws teach that there is a linear relationship between fluid flow rate and the pressure drop across a given conduit. As time progressed, however, it became obvious that both these Laws had limitations, and in the intervening 170 years approximately, much effort has been devoted to ascertaining the underlying reasons [5-12].Unfortunately, among practitioners, even to this day, there is much controversy regarding the parameters which constitute the pressure/flow relationship [13].

Darcy's original methodology used screened river sand packed into large pipes, through which he pumped water, and recorded the pressure drop across the packed pipe for each measurement of flow rate of the water [14]. It would be logical to conclude, therefore, that the precise nature of the sand particles, and the manner in which they were forced together inside the packed conduit, should be fertile ground for experimentation in any efforts to better understand the pressure/flow relationship in packed conduits [15].Throughout the middle to end of the 20th century, Blake, Kozeny, Carman, Bird Stewart and Lightfoot, Giddings, Halasz and Guiochon are just some of the more prominent scientists who devoted considerable effort to the elucidation of a fluid flow model capable of describing accurately the elements underlying this linear pressure/flow relationship, i.e., that portion of the fluid flow regime where viscous contributions to pressure drop dominate over kinetic contributions [16-22]. Unfortunately, however, their efforts did not culminate in a consensus of opinion and we are left today with the glaring contradictions regarding the value of the constant in the Kozeny/Carman equation, which is generally accepted as the most popular equation to describe the pressure/flow relationship in packed conduits, when the dominant contributions are derived

from viscous sources [23,24]. Giddings circa 1965, for instance, teaches that this value is 270 [25], Lightfoot circa 1960 teaches that its' value is 150 [19], while Halasz and his disciples claim that its value is 180 [26, 27], which is the value derived originally by Carman in 1937 [28]. Furthermore, the concept of conduit external porosity has been misapplied mostly in the engineering disciplines [29]. To make matters even worse, with the advent of the use of porous particles in applications like chromatographic separations, where solute molecules are separated based upon their ability to penetrate the pore network internal to the particles in a packed conduit, yet other elements of confusion have found their way into the controversy. Particle porosity, which is a variable that is independent of the packed conduit, has been invariably conflated with conduit internal porosity, and "mobile phase velocity", which is not a fluid velocity of any kind, has been conflated with the fluid velocity in many chromatographic journal publications [30, 31]. In the realm of the flow regime where kinetic contributions begin to manifest, Sabri Ergun circa 1950, in combination with others, most notably Orning, produced an equation which uses the sum of two distinct terms to capture both viscous and kinetic contributions [32]. This was a significant step forward in understanding how the pressure/flow relationship changes as the fluid accelerates into the region where kinetic contribution trump viscous contributions. Sadly, however, in 1952 this development morphed into, one step forward and two steps backwards, when Ergun assigned values of 150 and 1.75 for the constants in the viscous and kinetic terms in his now famous "Ergun equation" [33]. Throughout the intervening years, these values have been shown to be un-certifiable and, consequently, have added fuel to the fire of the ever-expanding controversy which litters this field of study to this very day [34].

While experimentation on packed conduits were in progress in the middle of the 20th century by the investigators mentioned above, other investigators, in parallel, were focused on the exact same objective with respect to the flow in empty conduits [35]. The efforts of Sir Osborn Reynolds, in particular, stand out, reaching back to 1883 [36]. Johan Nikuradze, for instance, is another most respected name when it comes to the fundamental experiments underlying the impact of inner wall roughness on the fluid flow profile in empty conduits. Actually, he carried out two seminal sets of experiments, circa 1933, one deals with smooth walled conduits and one deals with inner wall roughened conduits [37, 38]. Furthermore, since he was a student of Prandtl, their contributions are linked within a theory put forward by the latter, which forms the basis of their concept of the fluid boundary layer, a fluidic phenomenon that forms adjacent to a solid boundary due to viscosity, and which theory has been recognized as the father of wing flight fluid dynamics [39]. Fluid flow in empty conduits is extremely important in many engineering applications, so it is perhaps understandable that an engineer, Lewis Moody, circa 1944, building on the work of Nikuradze and others, produced the now famous "Moody diagram" which has been used as a popular "look up" chart by the engineering discipline for fluid flow designs which require knowledge of fluid flow in the region where kinetic contributions dominate [40]. The diagram is based upon the concept of "friction factor" which is a man-made entity, however, being as it is a mathematical construct and, thus, unfortunately, suffers from the defects of its qualities [41]. It has, in addition, been updated from time to time since its original creation [42]. In more modern times, the Princeton Super Pipe has gained in popularity with respect to the theory of fluid dynamics in smooth pipes and has been credited with an update to the conventional concept of the "Law of the Wall" [43].

It is apparent from the brief history of the development of fluid flow theory outlined above, that empty and packed conduits formed separate and distinct categories of investigative effort involving fluid flow theory throughout the past 150 plus years. While some attempts were made to produce a unified fluid flow model which would seamlessly embrace both types of fluid flow embodiments throughout that period, none were successful, at least up until now [44]. With the advent of the Quinn Fluid Flow Model (QFFM) published in 2019, this is no longer the case [45]. Accordingly, this paper is dedicated to elucidating a unified methodology for both packed and empty conduits, which a typical practitioner can take advantage of, whether that practitioner is an engineer, chromatographer or aerospace enthusiast.

2. Fundamentals of the Q Fluid Flow Model (QFFM)

2.1 Particle

Let us define an obstacle to be placed within a packed conduit as a spheroidal particle of nominal diameter d_{pm} and sphericity $\Omega_{p.}$ Then we may write:

$$d_p = d_{pm}\Omega_p \tag{1}$$

Where, d_p = the spherical particle diameter equivalent
$\Omega_p \leq 1$; thus, when $\Omega_p = 1$, the particle is spherical.

Let the particle have a specific pore volume of S_{pv}, a skeletal density of $\rho_{sk,}$ and a mass of m_p.

Let us define other particle characteristics as:

$$SA_p = \pi d_p^2 \tag{2}$$

And

$$CSA_p = \frac{\pi d_p^2}{4} \tag{3}$$

Where, SA_p = particle equivalent surface area; and
CSA_p = particle equivalent cross-sectional area.

It follows that we may write:

$$V_{dp} = \frac{\pi d_p^3}{6} \tag{4}$$

$$\rho_{part} = \frac{m_p}{V_{dp}} \tag{5}$$

Where, V_{dp} = the volume of a single spherical particle equivalent; ρ_{part} = the apparent particle density.

Let us define particle porosity as the ratio of free space within the particle to the total free space occupied by the particle as a whole, thus:

$$\varepsilon_p = S_{pv}\rho_{part} \tag{6}$$

Where, ε_p = the particle porosity.

It follows that:

When, $\varepsilon_p = 1$, the particle is devoid of solid matter, i.e., contains only free space;
When, $\varepsilon_p = 0$, the particle is made entirely of solid matter, i.e., the particle is non-porous;
When, $0 \leq \varepsilon_p < 1$, the particle is partially porous, i.e., consists of a solid particle skeleton plus internal pores.

2.2 Conduit

Let us define a fluid conduit as a right circular cylinder of length L and diameter D. Then we may write:

$$V_{ec} = \frac{\pi D^2 L}{4} \tag{7}$$

Where, V_{ec} = the volume of free space within an empty conduit.

Let the conduit be packed with n_p number of particle equivalents of diameter d_p.

It follows that we may write:

$$V_{part} = \frac{n_p \pi d_p^3}{6} \tag{8}$$

Where, V_{part} = the cumulative volume occupied by all the particle equivalents within a packed conduit.

Let us define as $n_{pq,}$ the number of particle equivalents whose collective volume is equal to the volume of free space within an empty conduit.

It follows that we may write:

$$n_{pq} = \frac{V_{ec}}{V_{dp}} = \frac{3D^2L}{2d_p^3} \tag{9}$$

Let us define the packed conduit fluidic architecture as:

$$\gamma = \frac{n_{pq}D}{L} \tag{10}$$

Where, γ = the fluidic architectural coefficient for a given packed conduit.

We now turn to conduit porosities.

Let us define the volume of free space within the packed conduit which is *external* to all the particles as V_e; the volume of free space which is *internal* to all the particles as V_i; the volume which is occupied by all the particle skeletons as V_{sk}; and V_t as the *total* volume of free space within the packed conduit which is devoid of solid matter.

It follows that we may write:

$$(1-\varepsilon_0) = \frac{n_p}{n_{pq}} = \frac{V_{part}}{V_{ec}} \tag{11}$$

Where, the conduit particle fraction, $(1-\varepsilon_0)$ = the volume fraction of the packed conduit occupied by the particles.

$$\varepsilon_{sk} = \frac{(1-\varepsilon_p)n_p}{n_{pq}} = \frac{V_{sk}}{V_{ec}} \tag{12}$$

Where, the conduit skeletal fraction, ε_{sk} = the volume fraction of the packed conduit occupied by the particle skeletons.

$$\varepsilon_0 = 1-\frac{n_p}{n_{pq}} = \frac{V_e}{V_{ec}} \tag{13}$$

Where, the conduit external porosity, ε_0 = the volume fraction of the packed conduit *external* to the particles.

$$\varepsilon_i = \varepsilon_p(1-\varepsilon_0) = \frac{V_i}{V_{ec}} \tag{14}$$

Where, the conduit internal porosity, ε_i = the cumulative volume fraction of the pores *internal* to the particles.

$$\varepsilon_t = 1-\frac{(1-\varepsilon_p)n_p}{n_{pq}} = \varepsilon_i + \varepsilon_0 \tag{15}$$

Where, the conduit total porosity, ε_t = the sum of the volume fraction of poress *external and internal* to the particles.

It follows that *particle* porosity and *conduit internal* porosity are related as follows:

when $\varepsilon_p = 0$, conduit internal porosity $\varepsilon_i = 0$ and, thus, the particles are completely solid throughout, i.e., non-porous.

when $\varepsilon_p = 1$, conduit internal porosity $\varepsilon_i = (1-\varepsilon_0)$ and thus, the particles are completely devoid of solid matter, i.e., totally porous.

Additionally, it follows that reconciling the definitions above for solid matter and lack thereof, i.e., porosity, within a conduit, [see Eqs. (8) and (11) above], we may now write:

$$\frac{n_p \pi d_p^3}{6} = V_{ec} abs(1-\varepsilon_0) \tag{16}$$

Equation (16) reconciles the distribution of free space within the conduit according to the conservation Laws of Nature, whereby all partial volume fractions of the fluid-filled packed conduit, whether occupied by solid matter or fluid, add to unity.

2.3 The Conservation Laws governing packed conduits

Thus, the Conservation Laws pertaining to packed conduits dictate that we may write:

$$\varepsilon_0 + \varepsilon_i + \varepsilon_{sk} = 1 \tag{17}$$

or

$$\varepsilon_t + \varepsilon_{sk} = 1 \tag{18}$$

Let us define the packing density of a packed conduit as:

$$\rho_{pack} = \frac{M_p}{V_{ec}} \tag{19}$$

Where, ρ_{pack} = the packing density of the packed conduit; $M_p = n_p m_p$, the total mass of all the particles in a packed conduit under study.

It follows that we may now write:

$$\varepsilon_0 = 1-\rho_{pack}(S_{pv}-1/\rho_{sk}) \tag{20}$$

or

$$\varepsilon_0 = 1 - [2n_p d_p^3/(3D^2L)] \quad (21)$$

Accordingly, we may write:

$$\varepsilon_p = \frac{(\varepsilon_t - \varepsilon_0)}{(1-\varepsilon_0)} \quad (22)$$

Substituting for the independently measured components of ε_p in Equation (22), gives

$$S_{pv}\rho_{part} = \frac{(\varepsilon_t - \varepsilon_0)}{(1-\varepsilon_0)} \quad (23)$$

It therefore follows that, empirically, we may define a packed conduit in terms of 4 *independent* variables (M_p, V_{ec}, S_{pv}, ρ_{sk}) or, alternatively, (n_p, d_p, D, L), *in combination with* one *dependent* variable (ε_0), all of which are *measurable*. However, if in addition to measuring the independent variables, one also measures the value of the external porosity, ε_0 (a dependent variable), both sides of equations (22) and (23) must be reconciled for any given packed conduit under study, *as dictated by the Conservation Laws* (sometimes referred to as the Laws of Continuity when their application involves moving entities like the fluid in this particular application). This dictate from the Laws of Continuity *trumps all measurement techniques,* which generally lack the specificity/accuracy to balance either equation without the need for further reconciliation or modification.

Thus, the lefthand side of equation (23) contains measurements made *outside* of the packed conduit, i.e., independent of the packed conduit under study, whereas the righthand side of equation (23) contains measurements made *within* the packed conduit under study. Accordingly, balancing of equation (23) is always necessary to validate the accuracy of the reported values for the measured parameters of the packed conduit under study.

It follows that, in the case of packed conduits which contain nonporous particles, equation (23) is equal to zero on both sides of the equalization sign, thus eliminating the need to reconcile column porosity and particle porosity.

2.4 The Q-Porosity Function (ε)

Let us now collect all the partial fraction (porosity) definitions in the QFFM underlying packed conduits which are defined in terms of particle size equivalents and view them as dimensionless mathematical functions of n_p, which we will designate as Q-Porosity functions. There is a total of 5 such functions, which we view in the context of the generalized Q-Porosity function ε.

1. $(1-\varepsilon_0) = n_p/n_{pq}$, Equation (11) above

2. $\varepsilon_{sk} = (1-\varepsilon_p)n_p/n_{pq}$, Equation (12) above

3. $\varepsilon_0 = (1-n_p/n_{pq})$, Equation (13) above

4. $\varepsilon_i = \varepsilon_p(n_p/n_{pq})$, Equation (14) above

5. $\varepsilon_t = 1- (1-\varepsilon_p)n_p/n_{pq,}$ Equation (15) above

It now becomes obvious that the Q-Porosity functions ε_0 and $(1-\varepsilon_0)$ are *independent* of the value of the particle porosity, ε_p.

Similarly, it is also obvious that the Q-Porosity functions $\varepsilon_{i,}$ ε_{sk} and ε_t are *dependent* on the value of the particle porosity, ε_p.

Note that when the value of $\varepsilon_p = 1$, the value of $\varepsilon_{sk} = 0$.

2.5 Solid Particles ($0 \leq \varepsilon_p < 1$)

Let us now define the conduit packing process in the case of solid particles ($0 \leq \varepsilon_p < 1$) by viewing the role of our independent variable, n_p, within the context of the Q-Porosity function (ε). This is best accomplished by viewing a worked example on a plot of the dimensionless Q- Porosity function, ε, versus the number of particle equivalents, n_p.

Our chosen worked example consists of 10 μ particles packed into a conduit of dimensions 10 cm in length and 0.46 cm in diameter, the details for which are presented in Figure 1, for the case in which the particles are nonporous ($\varepsilon_p = 0$).

As shown in Figure 1 below, our empirical packing process recognizes Kepler's conjecture regarding the stacking of solid spheres. Accordingly, the maximum value of the Q-Porosity function $(1-\varepsilon_0)$ is approximately 0.74 with the corresponding minimum value of approximately 0.26 for the Q-Porosity function $\varepsilon_{0.}$ Kepler's conjecture is a consequence of the fact that solid spheres and free space are *mutually exclusive* and therefore the maximum value of n_p achieved empirically must be less than the value of n_{pq}. The upper limit of the value of n_p is always n_{pq} since it represents the most particle equivalents, *theoretically*, that could be packed into any given conduit under study.

Accordingly, the theoretical *domain* of the Q-Porosity function (ε) runs from 0 to n_{pq} and the *ranges* of the function vary between the values of 0 and 1, as shown in Figure 1.

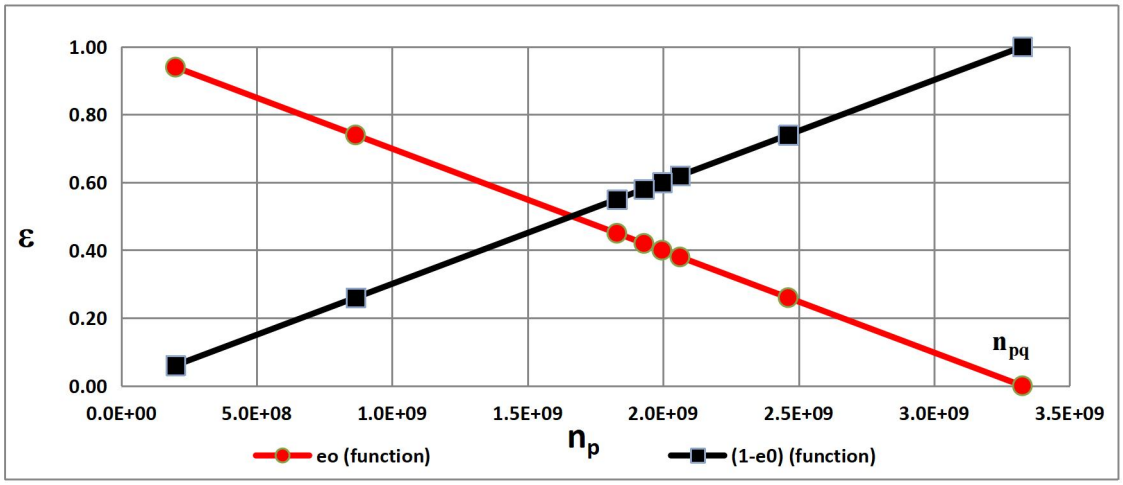

Figure 1 Q-Porosity Function for Non-Porous Particles ($\varepsilon_p = 0$)

In Figure 1 we only display two of the Q-Porosity functions, i.e., ε_0 and $(1-\varepsilon_0)$, since they are not influenced by the particle porosity value, ε_p, and, in this particular case ($\varepsilon_p = 0$), $\varepsilon_i = 0$, $\varepsilon_t = \varepsilon_0$ and $\varepsilon_{sk} = (1-\varepsilon_0)$. Additionally, we note that these two functions are *reciprocal* in nature to the extent that as one increases, the other decreases, all as a function of n_p.

We now further refine the definition of the entity $\mathbf{n_p}$ to be that of a *vector* rather than a *scalar* quantity and, therefore, *confer upon it a directional component* in addition to its mandatory *magnitude* component.

Let us now define the *packing process of a conduit*, using our example with solid particles, in terms of our mathematical Q-Porosity functions, as the direction of increasing *positive* values of n_p. Thus, as we move along the x axis of Figure 1 in the direction of left to right, starting at the origin of the plot at $\mathbf{n_p} = 0$, the corresponding values on the y axis represent the changing characteristics of the Q-Porosity function ε in the filling (packing) process. At the starting point of $\mathbf{n_p} = 0$, the conduit is devoid of particles (contains only free space) and at the maximum value of $\mathbf{n_p}$ achieved in the filling process, the conduit is fully packed. Accordingly, filling of a "packed" conduit with solid particles is represented by the increasing positive values of $\mathbf{n_p}$, i.e., the motion left to right along the x axis of the plot starting at the value of $\mathbf{n_p} = 0$ →.

We shall now consider the more complex packing process in which the particle porosity varies between the values of 0 and 1, i.e., the case of partially porous particles ($0 < \varepsilon_p < 1$).

In our worked example shown in Figure 2, we show as our example a packed conduit with particles which have a particle porosity of 0.6 ($\varepsilon_p = 0.6$). Because the porosity functions of ε_i, ε_t and ε_{sk} are dependent on the value of ε_p, we include these functions in our Figure 2.

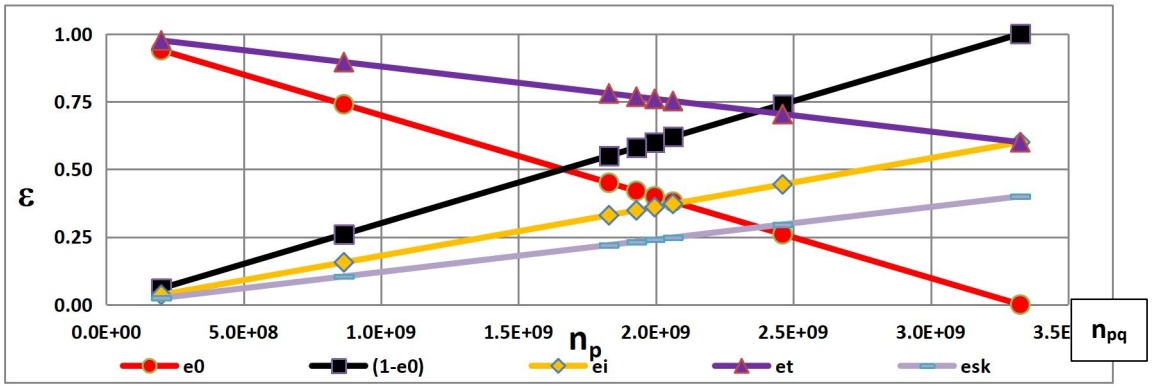

Figure 2 Q-Porosity Function for Partially Porous Particles ($0 < \varepsilon_p < 1$)

As displayed in Figure 2, each of the 5 Q-porosity functions, ε_0, $(1-\varepsilon_0)$, ε_i, ε_t, and ε_{sk} have discrete and different values for all values of $\mathbf{n_p}$.

2.6 Hypothetical Q-Particles ($\varepsilon_p = 1$)

We shall now consider the packing process in the *special case* when the particles are *fully* porous, i.e., they are completely made of free space ($\varepsilon_p = 1$). This scenario is presented in Figure 3.

As shown in Figure 3, our packing process for particles made of free space ($\varepsilon_p = 1$), which we designate as hypothetical Q-particles, is represented by increasingly *negative* values of $\mathbf{n_p}$. Accordingly, the domain of the Q-Porosity function runs from 0 to - n_{pq}. Similarly, it follows that the range of the function varies between the values of -1 and 2, as shown in the plot.

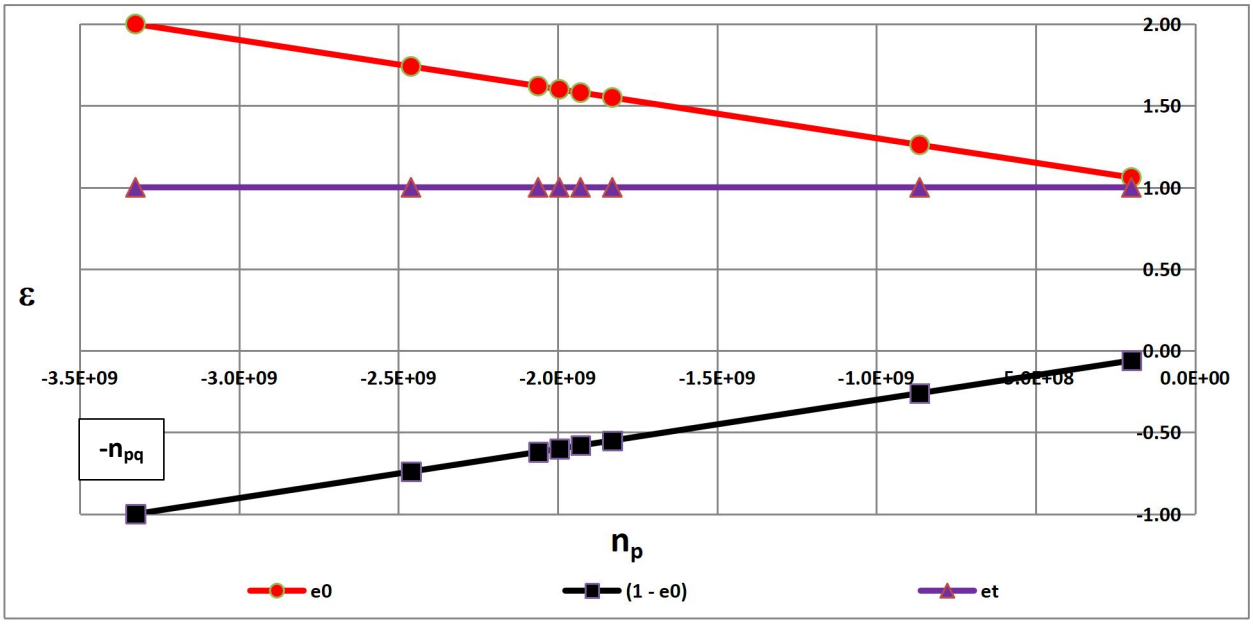

Figure 3 Q-Porosity Function for Fully Porous Particles ($\varepsilon_p = 1$)

In this scenario the Q-Porosity functions $\varepsilon_t = 1$ and $\varepsilon_{sk} = 0$ for all values of $\mathbf{n_p}$. The function ε_i has identical values to the function $(1-\varepsilon_0)$ and varies between 0 and -1, whereas the value of the function ε_0 varies between 1 and 2.

Let us now define the directional component of packing a conduit with hypothetical Q-particles in terms of our mathematical Q-Porosity functions. As we move along the x axis of Figure 3 in the direction of right to left, starting at the origin of the plot at $\mathbf{n_p} = 0$, the corresponding values on the y axis represent the changing characteristics of the Q-Porosity function ε in the filling (packing) process. This direction of filling is the opposite of that for solid particles. At the starting point of $\mathbf{n_p} = 0$, we consider the conduit to be devoid of all particles (including particles of free space) and at the maximum value of $\mathbf{n_p} = -n_{pq}$ achieved in the filling process, the conduit is fully packed with particles of free space (hypothetical Q-particles). Accordingly, filling of a "packed" conduit with hypothetical Q-particles is represented by increasing negative values of $\mathbf{n_p}$, i.e., the motion right to left along the x axis of the plot starting at $\mathbf{n_p} = 0 \leftarrow$.

It follows that in the case of hypothetical Q-particles which are made of free space, Kepler's conjecture does not apply, since particles of free space are *mutually inclusive* with free space, i.e., they *are* free space. Accordingly, the maximum value of $\mathbf{n_p}$ achieved empirically is $-n_{pq}$, which corresponds to the conduit being filled with free space, and is also the upper *theoretical* limit of $\mathbf{n_p}$ in these circumstances.

We choose to use, advantageously, the *absolute value* of the porosity function $(1-\varepsilon_0)$ in our theoretical development, which represents the *magnitude* of the function and is, therefore, always positive, as shown in Figure 4.

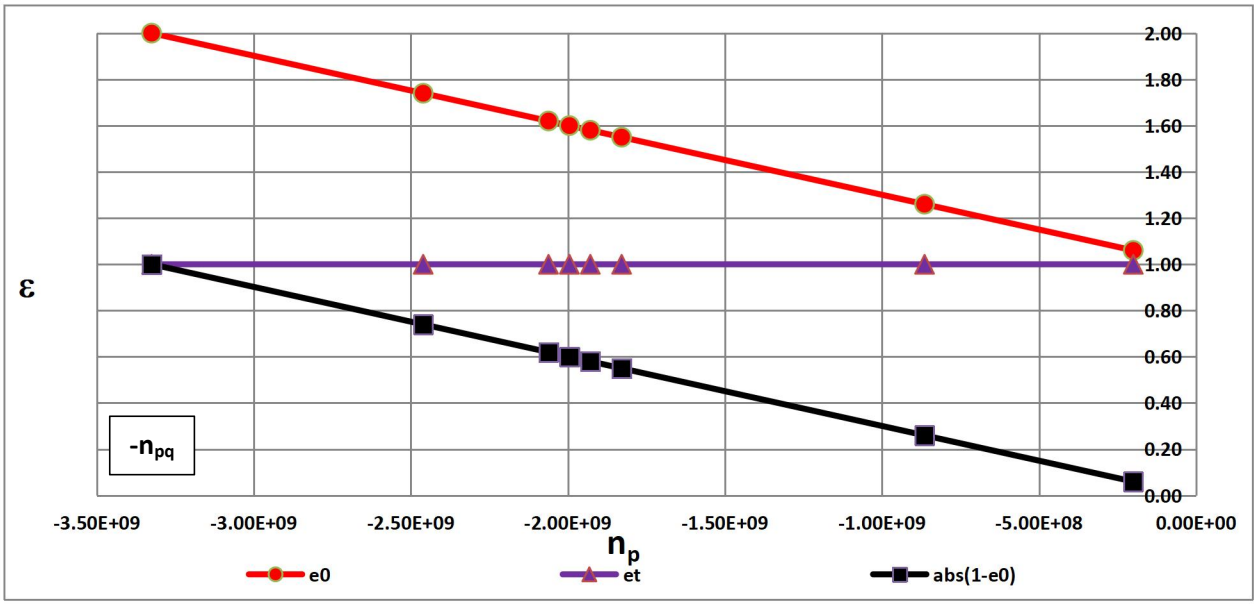

Figure 4 Q-Porosity Function for Fully Porous Particles ($\varepsilon_p = 1$)

Accordingly, as shown in Figure 4, the *range*s of all Q-Porosity functions *of interest* in this special case have positive magnitudes, and vary between the values of 0 and 2.

2.7 The Packed Conduit Hypothetical Q Channel Defined

Let us define a hypothetical *cylindrical* fluid channel within a packed conduit, which we shall call the hypothetical Q channel (HQC), whose characteristic dimensions are defined as:

$$d_c = \frac{d_p}{abs(1-\varepsilon_0)} = \frac{d_p}{abs(n_p/n_{pq})} \tag{24}$$

Where, d_c = the diameter of the HQC.

It follows that we may write [see Eqs. (7) and (14)]:

$$v_c = V_{ec}\varepsilon_t = \frac{\pi n_{pq} d_p^3 \varepsilon_t}{6} \tag{25}$$

Where, v_c = the volume of the HQC.

It follows that we may also write:

$$a_c = \frac{\pi d_c^2}{4} = \frac{\pi n_{pq}^2 d_p^2}{4 n_p^2} \tag{26}$$

Where, a_c = the cross-sectional area of the HQC.

Similarly, we may write:

$$l_c = \frac{v_c}{a_c} = \frac{2 n_p^2 d_p \varepsilon_t}{3 n_{pq}} \tag{27}$$

Where, l_c = the length of the HQC.

Let us define the Unit Hypothetical Q Channel as a *special case* of the more general HQC. It is defined as a conduit filled with hypothetical Q-particles having two *fixed* boundary conditions: (1), $d_p = D$ and (2), $n_p = -n_{pq.}$

It follows that, since the function $\varepsilon_0 = 2$ when $n_p = -n_{pq}$, the function $abs(1-\varepsilon_0) = 1 = \varepsilon_t$.

Accordingly, any "empty" conduit/capillary is represented in the QFFM by what we now term the Unit HQC since, by definition, its Q-Porosity functions of [abs $(1-\varepsilon_0)$] and ε_t are unity, as shown below in table 4 for our worked example.

As shown in Figure 5 below, any conduit/capillary when <u>totally filled</u> with hypothetical Q-particles ($n_p = -n_{pq}$), whose diameters are equivalent to the diameter of the conduit ($d_p = D = d_c$), will *always* have the *constant* values shown below, regardless of what the conduit dimensions are.

Thus, an empty conduit/capillary is defined in the QFFM as a packed conduit containing hypothetical particles with a particle porosity of unity ($\varepsilon_p = 1$), and is represented by the Unit HQC with the following *constant* values:

$\varepsilon_p = 1$; $n_p = -n_{pq}$; $d_p = D = d_c$; $l_c = L$; $v_c = V_{ec}$; abs$(1-\varepsilon_0) = 1$; $\varepsilon_0 = 2$; $\varepsilon_t = 1$; $\delta = 0.125$ (1/8); $\gamma = 1.5$ (3/2); $\tau = 0.188$ (3/16).

To further articulate the characteristics of the Unit HQC in the case of our chosen worked example, we present here 4 graphical representations of the primary channel functions; see Figures 5, 6, 7 and 8.

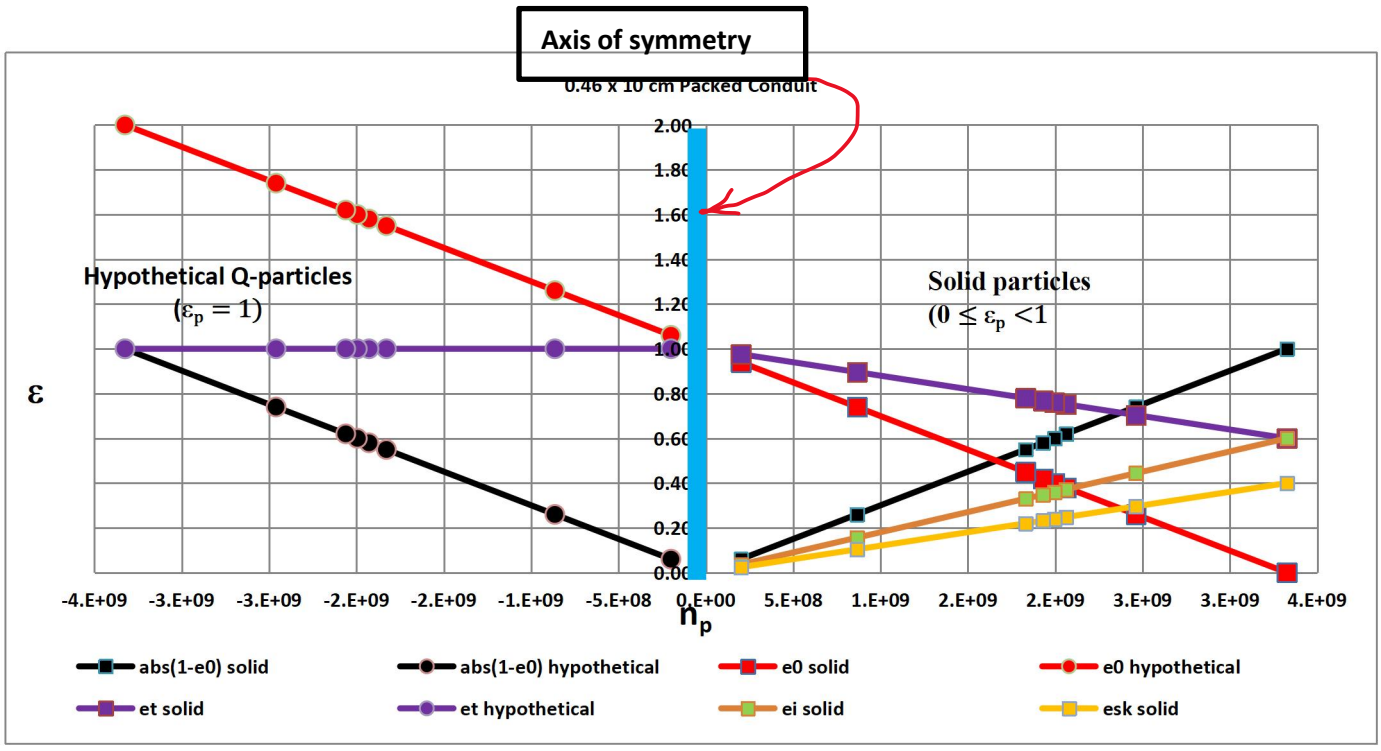

Figure 5 The HQC (Q-Porosity Function)

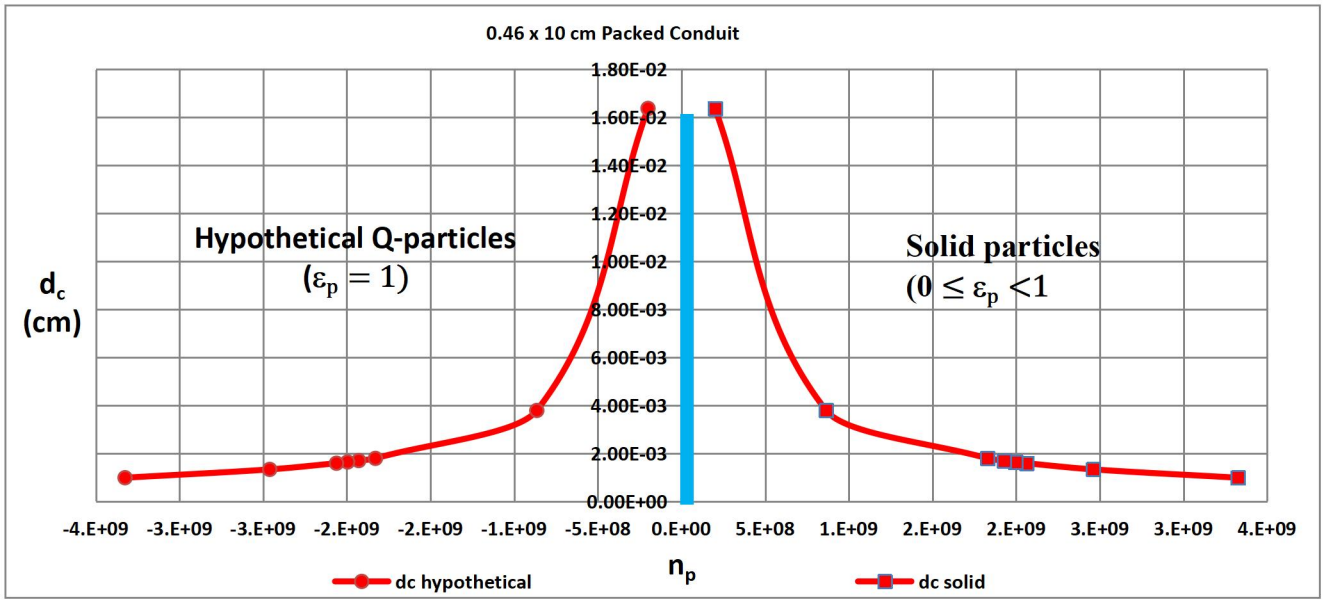

Figure 6 The HQC (dc function)

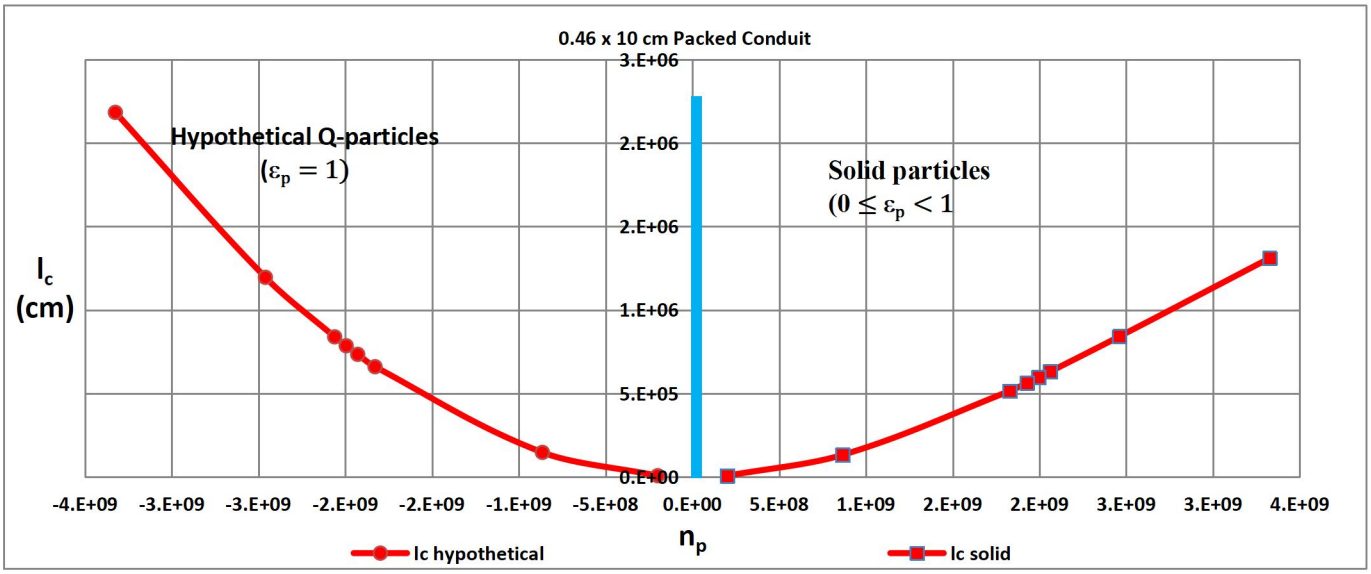

Figure 7 The HQC (l_c function)

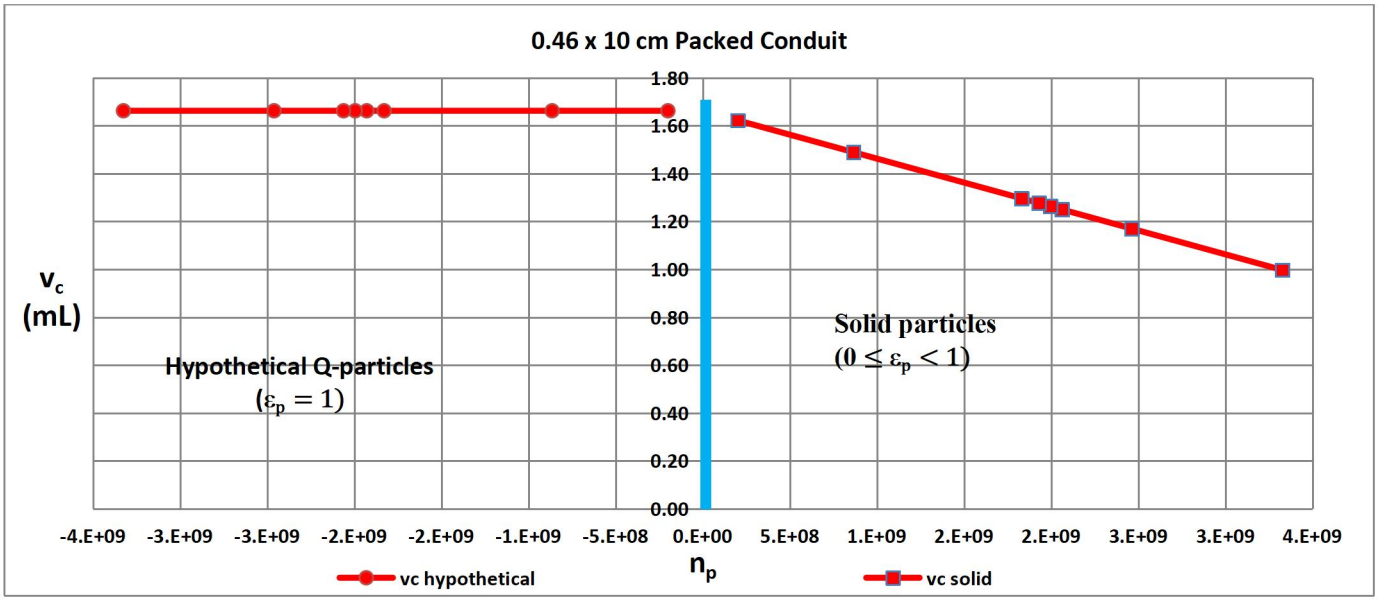

Figure 8 The HQC (v_c function)

As shown in Figure 5, the vertical line in the range of the Q-Porosity function (ε), ι.ε., $n_p = 0$, represents the axis of symmetry between the half-plane Q-Porosity function for solid particles, on the one hand (right hand side half-plane), and hypothetical Q particles, on the other hand (left hand side half-plane). Therefore, each of the mathematical half-planes is the mirror image of one another. Note that the Q-Porosity functions are *discontinuous* at the value of $n_p = 0$, the axis of symmetry, but are *continuous* at all other values of $\mathbf{n_p}$, i.e., $-n_{pq} \leq n_p < 0$; $0 < n_p \leq n_{pq}$.

It follows that, as shown in Figure 6, the HQC function d_c is correspondingly discontinuous at the value of $n_p = 0$, since at this precise value the *diameter* of the HQC tends to infinity. Thus, in the QFFM, the "infinite diameter packed conduit" is prohibited by hypothesis.

Finally, it follows that, as shown in Figure 7, the HQC function l_c is zero at the value of $n_p = 0$. In addition, the value of l_c is always greater for values of n_p less than zero, than for values of n_p greater than zero, a consequence of a value for external porosity in excess of unity, in this half-plane of the function.

Similarly, it follows that, as shown in Figure 8, the HQC function v_c is correspondingly discontinuous at the value of $n_p = 0$, since at this precise value, the volume of the HQC is *undefined,* but at all values of n_p less than zero, its volume is a *constant* positive value and at all values of n_p greater than zero, it has a *variable* positive value.

Finally, it is now obvious that in an empty conduit the Q-porosity conduit function of ε_i becomes part of the Q-porosity function ε_0 and there is no particle skeleton fraction.

3. Methodology

We begin by introducing a methodology used in engineering circles called Hydraulic Conductivity [46]. To put this term in context for all disciplines, we show the relationship between hydraulic conductivity ($\Delta H/L$) and pressure gradient ($\Delta P/L$):

$$\frac{\Delta H}{L} = \frac{\Delta P}{\rho_f g L} \tag{28}$$

We can see from the righthand side of equation (28) that hydraulic conductivity involves, not only, the pressure gradient across a packed conduit, but also, includes the additional variable, ρ_f, the fluid density, and g, the acceleration due to gravity. Thus, from an empirical perspective, a practitioner need only measure the pressure drop at any given flow rate, the length of the conduit, and obtain from reference text books the value for the density of the fluid used in the measurement, as well as the acceleration due to gravity. In addition, since it is customary when carrying out permeability determinations in packed conduits, to record the measured flow rate corresponding to the measured pressure drop, as fluid flux through the packed conduit, plotting fluid flux versus hydraulic conductivity is a popular engineering methodology. Thus, we can write:

$$\mu_s = \frac{4q}{\pi D^2} \tag{29}$$

Where, μ_s = fluid flux, also called linear superficial fluid velocity, q = volumetric fluid flow rate, D = the conduit diameter.

Accordingly, in order to use the fluid flux parameter, the practitioner must measure, in addition to the fluid volumetric flow rate, the conduit diameter.

When reporting empirical results of permeability in packed conduits, the Forchheimer fluid flow model is a popular engineering methodology, especially when the fluid flow regime involves significant kinetic contributions [47]. We can write the Forchheimer equation as follows:

$$\frac{\Delta H}{L} = a\mu_s + b\mu_s^2 \tag{30}$$

Where, a, and b, are the Forchheimer coefficients for the viscous and kinetic contributions, respectively.
Thus, we can see from equation (30) that hydraulic conductivity is a quadratic function of fluid flux. It is customary in engineering circles to make a plot of equation (30), a typical example of which is shown in Figure 9.

Figure 9. Hydraulic conductivity as a quadratic function of fluid flux.

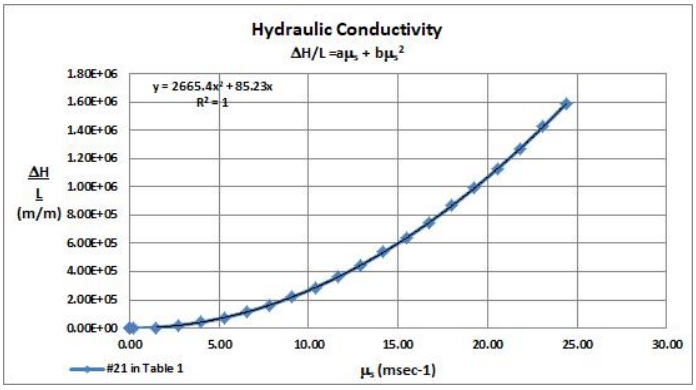

Figure 9 Hydraulic Conductivity

As shown in Figure 9, the second order polynomial trend line associated with this plot renders the values of a, and b, both of which are represented as having a constant value, over all flow rate ranges (50).

3.1 Anatomy of the QFFM

Th QFFM applies to all fluid flow regimes. Specifically, it provides a detailed analytical definition of the fluid flow parameters which make up the numerical values of a, and b, for any experiment under study. Thus, we provide, herein, the definition for a, and b, as taught by the QFFM:

$$a = \frac{4r_h^3\pi\delta\eta}{3\rho_f g d_c^2} \tag{31}$$

$$b = \frac{\delta^2\lambda}{2\pi g d_c} \tag{32}$$

In addition, the QFFM also provides all the needed relationships between the measurable fluid flow embodiment parameters necessary to completely establish the fluid flow relationship. Thus, we include some additional pertinent equations herein:

$$\delta = \frac{1}{\varepsilon_0^3} \tag{33}$$

$$\varepsilon_0 = 1-\frac{n_p}{n_{pq}} = 1-\frac{2n_p d_p^3}{3D^2L} \tag{34}$$

$$n_{pq} = \frac{3D^2L}{2d_p^3} \tag{35}$$

$$d_c = \frac{d_p}{abs(1-\varepsilon_0)} \tag{36}$$

$$\lambda = (1+W_N) \quad (37)$$

where, r_h = fluid drag normalization coefficient, i.e., 4, η = the fluid absolute viscosity, d_p = the spherical particle diameter equivalent, d_c = the diameter of the hypothetical Q-channel, n_p = the number of particles in the packed conduit under study, and λ = the normalization coefficient for wall effects, generally equal to unity for packed conduits.

Since the parameter λ, however, involves a very complex definition involving many different independent and dependent variables, it is beyond the scope of this paper and, consequently, we refer the reader to the original publication the QFFM for all the details concerning the components of λ [45]. Additionally, for the reader's convenience, we have included in the addendum to this paper, a comprehensive reference guide which provides, nomenclature, glossary of terms and all formulae from the original publication of the QFFM.

3.2 Solving the Navier-Stokes Equation for Closed Conduits

The QFFM is the only extant theory of fluid dynamics which includes an equation capable of describing the relationship between fluid flow rate and pressure drop that is unique in its ability to describe, accurately and precisely, this relationship throughout the entire fluid flow regime, including all three so-called regions of laminar, transitional and fully turbulent. This includes all the elements of "wall effects" both primary and secondary. We shall now explore in detail how this is accomplished.

1. Definition of Parameters.

The QFFM teaches that there are 17 important parameters in the pressure flow relationship in closed conduits, representing 3 distinct categories which include: (a) constants, (b) independent variables and (c) dependent variables:

a. There are 4 constants:

π, r_h, k_1 and k_2

b. There are 9 independent variables:

3 Fluid variables: η, ρ_f and q.

4 Packed conduit variables: D, L, n_p, and k.

2 Particle variables: d_{pm}, Ω_p,.

c. There are 4 dependent variables:

1 Fluid variable: $\lambda = f(\pi, r_h, R_{em}, k, \delta,)$

3 Packed conduit variables: $d_p = f(d_{pm}, \Omega_p)$,

$\varepsilon_0 = f(\pi, D, L, d_p)$,

$$\Delta P = f(\lambda)$$

2. Formula

The QFFM formula can be written as:

$$P_Q = k_1 + k_2 C_Q, \tag{38}$$

which is the dimensionless manifestation of Quinn's Law and is a unique formula which combines the above identified variables in a manner never before contemplated.

3. Underlying theory

What makes the QFFM unique is that it contains many parameters not identified in other fluid dynamic models, i.e., r_h, k_1, k_2, β_0, τ, λ, Q_N, C_Q, etc., etc., and, in addition, combines all the parameters in a unique arrangement not heretofore available in any other fluid model.

Thus, when the fluid flow rate, pressure drop and conduit diameter are determined by experiment and, accordingly, the Forchheimer values of a, and b, are known, based upon accurate measurements of these three variables over a broad range of flow rates, including the non-linear region, where kinetic contributions to measured pressure drop are significant and, in combination with the fluid property of kinematic viscosity, we can solve the N-S equation using the QFFM. Thus, we proceed as follows:

It follows from equation (31) above that we may write:

$$\frac{\delta}{d_c^2} = \frac{3a\rho_f g}{4r_h^3 \pi \eta} \tag{39}$$

Similarly, it follows from equation (32) above that we may write:

$$\frac{\delta^2}{d_c} = \frac{2b\pi g}{\lambda} \tag{40}$$

Therefore, in order to solve the N-S equation we must satisfy both equations (39) and (40) *simultaneously*.

From equation (39), let us assume that:

$$\frac{\delta}{d_c^2} = \alpha \tag{41}$$

From equation (40), let us assume that:

$$\frac{\delta^2}{d_c} = \beta \tag{42}$$

Let us further assume that:

$$x = \alpha\beta \tag{43}$$

Similarly, let us assume that:

$$y = \frac{\alpha}{\beta} \tag{44}$$

It follows that we may now write the solution to the N-S equation for closed conduits as:

$$d_c = \frac{1}{x^{(1/6)}y^{(1/2)}} \tag{45}$$

$$\delta = \frac{x^{(1/6)}}{y^{(1/2)}} \tag{46}$$

The above simultaneous solution for the values of d_c and δ depends, not only, upon the independent variables identified above, but also, upon the value of λ in equation (32). However, λ, in turn, depends upon the value of other variables including d_c, a dependent variable itself and, accordingly, and problematically, this is the conundrum of solving the N-S equation. Furthermore, the variable ε_0 (conduit external porosity), is clearly the most important variable amongst all the variables in the pressure flow relationship, since it appears in both the Forchheimer coefficients a, and b (equations (31) and (32)), and is also present in equations (45) and (46). *Additionally, there is no more sensitive relationship in all of physics between the value of ε_0 in the Forchheimer coefficient b, and the value of the pressure gradient $\Delta P/L$, when the fluid flow profile contains significant kinetic contributions.*

Therefore, the QFFM is the only fluid flow model in existence today that can return a valid analytical solution, based upon pressure drop and flow rate measurements, for the values of d_c and δ, simultaneously, for any given flow rate, in any given experiment, in a closed conduit, regardless of whether that conduit is packed with particles or empty, and regardless of where in the fluid flow regime that flow rate may fall, laminar, transitional or fully turbulent. This unequivocal assertion is a manifestation of the solution to the N-S equation for fluid flow in closed conduits packed with chromatographic particles (HPLC).

3.3 Executing the QFFM solution to N-S equation

The QFFM provides the means by which one can overcome this fluid dynamic conundrum in solving the N-S equation for closed conduits, by establishing an understanding of the value of λ under three distinct closed conduit milieus, two of which are self-evident, based upon the underlying theory, and one of which necessitates an additional measurement of an independent variable.

We digress here to emphasize that the parameter λ, as defined in the QFFM, is bounded on the lower side by an asymptote which tends to the value of unity when the packed conduit tortuosity term, τ, is very large. The definition of the conduit tortuosity term τ, in turn, is based upon the architectural makeup of the particular closed conduit under study. It is, therefore, a totally novel concept for this parameter, amongst all other existing and competing theories of fluid dynamics. Consequently, the concept of conduit tortuosity, as defined in the QFFM, is what differentiates the fluid dynamics within different closed conduits and, accordingly, defines the three distinct closed conduit milieus regarding the values of λ, which arise in the case of fluid flow in packed and empty closed conduits. These distinct milieus may be catalogued as follows:

1. Packed conduit with low value of the ratio D/d_p

The most general case of a packed conduit is when the ratio of D/d_p is low, say less than 10. In this scenario, the QFFM teaches that there is a significant primary wall effect at very low values of the modified Reynolds number and, consequently, the value of λ will not be exactly equal to 1.0 and, together with the value of the Forchheimer coefficient b, will vary based upon the fluid velocity used in any experiment under study.

It is important to understand, however, that in this milieu, even though the primary wall effect is significant at very low values of the modified Reynolds number, it will only manifest in the pressure gradient measurements at moderate values of the modified Reynolds number. This is because all wall effects, and therefore the λ parameter, manifests only in the kinetic term, which has a relatively small contribution to the measured pressure gradient at very low values of the modified Reynolds number. One could, theoretically, make measurements at very high modified Reynolds number values, where the value of λ would tend to unity as the boundary layer is dissipated, but this could require large pressure drops, not practical in a typical practitioner's laboratory. Therefore, alternatively, one must know, in addition to the values of the Forchheimer coefficients a, and b, at least one more independent variable, to solve the N-S equation in this milieu scenario at reasonable pressure drops. **That independent variable is n_p, the number of particles in any packed conduit under study, which must be independently measured in this scenario of a packed conduit.** Again, we point out that in this scenario, the plotting techniques using equation (30) will not produce accurate values for the Forchheimer coefficients a, and b.

Thus, the QFFM is the only model capable of validating the accuracy and precision of the underlying conduit variables of d_p, and ε_0, based upon Forchheimer type measurements of fluid flux and hydraulic conductivity,

and which also include an independent measurement of the value of n_p, in this milieu, where the primary wall effect is significant at low to moderate flow rates.

2. Packed conduit with smooth particles and a large value of the ratio D/d_p

A packed conduit where the ratio of D/d_p is large, say greater than 30. This represents a special boundary condition in the application of our solution. In this scenario, the QFFM teaches that there is no primary wall effect, because the value of the packed conduit tortuosity term, $\tau = \delta\gamma$, is very large and when the particles are smooth, there is no secondary wall effect. Accordingly, the measured values for the Forchheimer coefficients a, and b, will both be constant at all fluid velocities. Thus, the above solution for the values d_c and δ is absolute at a value of $\lambda = 1$, since in equation (32), all the values of the parameters are uniquely defined at this boundary condition. This is typically the case for most commercially available packed conduits, including most HPLC columns, since they are typically designed with large ratios of D/d_p for performance related reasons. In this scenario, the technique outlined above of identifying the values of the Forchheimer coefficients a, and b, by plotting equation (30) will yield accurate values across the full spectrum of modified Reynolds number, **if sufficient flow rate measurements are taken both in the linear and non-linear regions of the flow regime, which includes the region in which kinetic contributions to the measured pressure drop are significant. Thus, in this new teaching, measurements which include kinetic contributions are critical to identify an accurate value of the Forchheimer coefficients a, and b, regardless of what flow regime a particular experimental protocol may be focused, i.e., permeability studies in the laminar regime are included in this qualification which is the case with most HPLC columns.**

We emphasize that in the literature for packed conduits in many applications, and especially in the field of chromatography, kinetic contributions to measured pressure drop have been totally ignored in favor of just doing measurements in the laminar regime. This results in inaccurate values for the Forchheimer coefficients a, and b, which, in turn, means that studies carried out under this set of experimental protocols will not facilitate validation of any underlying packed conduit variables. Indeed, when other fluid flow models are used in this scenario, such as the popular Kozeny-Carman model, in the case of packed conduits containing solid particles, and the Hagen-Poiseuille model, in the case of empty conduits, to back-calculate either the value of D, d_p or ε_0, they will provide only crude estimates of the true value of these parameters.

3. Empty conduits

All empty conduits regardless of the independent variable values which define them, i.e., the conduit diameter, D, the conduit length L, or the inner conduit wall roughness k, represent another special case of a packed conduit in the QFFM. Thus, although the QFFM teaches that an empty conduit has a relatively low tortuosity value and, consequently, a large value for λ at low flow rates, this is offset by the fact that its value is always constant, i.e.,$\tau = 3/16$, which is a consequence of *four limiting boundary* conditions for an empty conduit: (a) $d_p = D$, (b) $\delta = 1/8$, (c) $n_p = -n_{pq}$, and (d) $\varepsilon_p = 1$, where ε_p represents the *particle* porosity (not to be confused with ε_i, the *conduit*

internal porosity), and when its value is unity, as in the case of an empty conduit, represents particles of free space. Thus, in an empty conduit, which corresponds to a packed conduit filled with particles of free space, there is less degree of freedom than in a packed conduit filled with particles which have a solid skeleton. This boundary condition, in turn, results from the Laws of Nature which dictate that solid matter and free space are mutually exclusive. It follows, therefore, that the values of λ, d_c, δ in equation (40) will be uniquely defined when these four boundary conditions prevail. Thus, setting four boundary conditions in the QFFM for the values of $\delta = 1/8$, $d_p = D$, $n_p = -n_{pq}$ and $\varepsilon_p = 1$, establishes a unique value for λ at any given flow rate, when the Forchheimer type coefficients a, and b, are known. We emphasize, however, that the technique outlined above of using plots of equations (30), as shown in Figure 9, will not produce accurate values for the Forchheimer coefficients a, and b, in the case of an empty conduit, since they are only capable of returning an average value for these coefficients and, of course, the value of b in an empty conduit varies as a function of flow rate.

Thus, the QFFM is the only fluid flow model capable of validating the accuracy and precision of the underlying conduit variables of D, L, and k, in an empty conduit, based upon Forchheimer type measurements of fluid flux and hydraulic conductivity.

We digress, once again, to explain the significance of the QFFM as it pertains to the independent variable, k, the roughness of the inner conduit wall in an empty conduit. There are just three variables for an empty conduit, D, L, and k. The former two variables are easy to measure and, in addition, can usually be measured with a high degree of accuracy. This is not the case with the latter variable, k which is very difficult to measure, in the first instance, not to mention the accuracy of the measurement. Accordingly, in the case of an empty conduit, one can use the Forchheimer equivalent type measurements for an empty conduit, in conjunction with the QFFM, to accurately back-calculate for the value of k, when the measured data contains pressure drop measurements taken at sufficiently high values of the modified Reynolds number, where the secondary wall effect, i.e., the wall roughness coefficient, manifests itself by punching through the ever- dissipating boundary layer. *This is a very effective tool for the practitioner.*

Finally, to help visualize how all this information comes together in the QFFM, we show in Figure 10 a plot of dimensionless permeability Θ versus fluid current Q_N over 11 orders of magnitude of R_{em}.

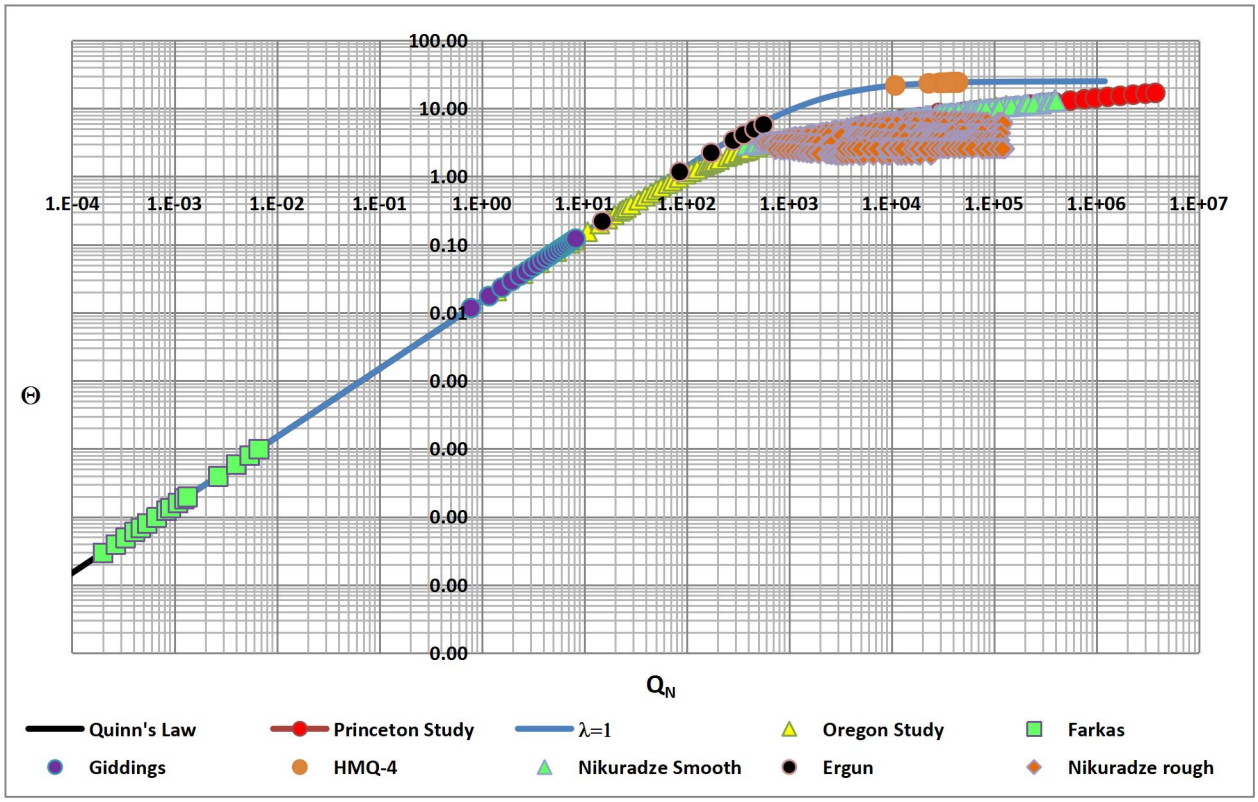

Figure 10 Dimensionless permeability

As shown in Figure 10, published data for both conduits packed with solid particles and empty are displayed in the same frame of reference. Note that packed conduits are differentiated from smooth walled empty conduits and, in turn, roughened walls empty conduits.

4. Validation

The QFFM, by virtue of its ability to accommodate seamlessly both types of conduits, i.e., empty and packed with solid particles, enjoys the unique characteristic of being certifiable over the entire fluid flow regime, from creeping flow to fully developed turbulence. This is because conduits packed with solid particles can be validated at very low modified Reynolds numbers, whereas empty conduits can be validated at very large modified Reynolds numbers. This, in turn, is a consequence of operating pressure drops. Accordingly, in Figure 11 we show validation of the QFFM over 11 orders of magnitude of the modified Reynolds number.

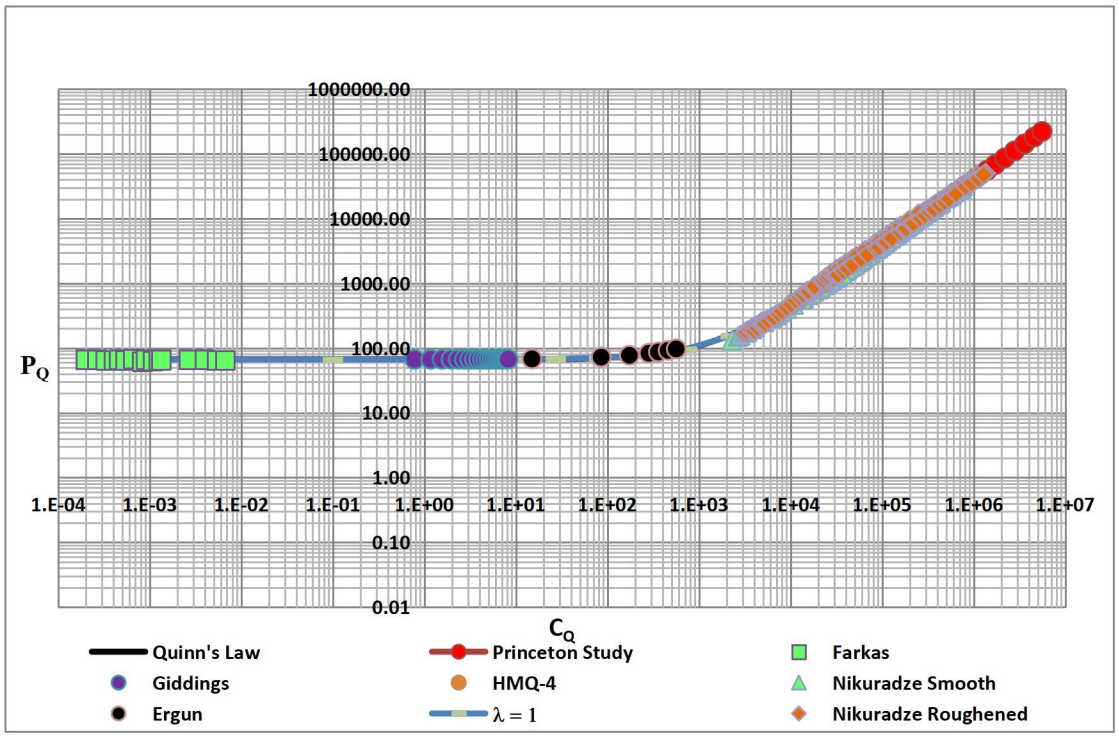

Figure 11 Quinn's Law Validation

As shown in Figure 11, the data of Farkas et al validates the QFFM at extremely low values of R_{em}, whereas the data of the Princeton Super Pipe study validates it at very high values of R_{em}. In addition, this plot also demonstrates that the measured data of all flow embodiments, conduits both empty and packed with solid particles, collapse onto the same straight line whose intercept on the y axis and slope of the line, represent the value of k_1 and k_2, respectively, in equation (38), i.e., Quinn's Law. The axes of the plot are log-log to show the extremes at both ends of the R_{em} values.

5. Conclusions.

In this paper, we have demonstrated a unique "solution equivalent" to the Navier-Stokes equation for closed conduits, expressed in terms meaningful to a chromatographer who may not be versed in advanced mathematics. In so doing, our conclusions can be catalogued as follows:

1. The value of the coefficient A in the re-invented Ergun model, i.e., the Q-modified Ergun equation, has the constant value of $256\pi/3$ which is 268.19 approx.
2. The value of the coefficient B in the re-invented Ergun model, i.e., the Q-modified Ergun equation, is a variable function of the external porosity of the conduit as well as the wall normalization coefficient λ.
3. The value of B falls in a range from 1.5 to 3.5 for well-packed conduits packed with rigid particles having a solid skeleton and a large ratio for D/d_p.

4. The value of B for an empty conduit has the constant value of 0.125 (1/8).

5. There is but one unique combination of values for d_p, ε_0 and n_p which will correlate permeability measurements over the entire range of the fluid flow profile, from creeping flow to fully turbulent flow. This is a result of the Laws of Nature which dictate that for any given conduit under study, every combination of the packed conduit values of the variables d_p and n_p represents a unique hypothetical Q channel and, consequently, a unique pressure gradient/fluid flow rate profile over the entire fluid flow regime.

6. The Conservation Laws dictate that for any given conduit dimensions, i.e., diameter D and length L, packed with rigid particles of spherical particle diameter equivalent, d_p, the value of ε_0, is not an independent variable but is defined by the combination of the values of d_p and n_p, i.e., the number of particles present in the packed conduit.

7. In order to accurately define the Forchheimer coefficients a, and b, empirical measurements must be taken in the nonlinear portion of the fluid flow regime, i.e., where kinetic contributions are significant. This is a result of the fact that kinetic contributions are much more sensitive to the value of the external porosity parameter, ε_0, than are viscous contributions. This prerequisite in determining the value of ε_0 has not been recognized in chromatography circles up to this point in time.

8. In most examples studied in the literature, including HPLC columns, the experimental protocols typically used to measure the values of d_p and ε_0 are not sufficiently accurate or precise to validate the value of these variables using pressure drop/flow rate measurements. Thus, the values reported in the literature have values for external porosity which are both too high and too low.

9. The QFFM teaches that when an empty conduit is considered as a conduit packed with particles of free space, i.e., $\varepsilon_p = 1$, there is an apparent increase in the magnitude of the value for the conduit external porosity ε_0. This apparent increase results from the phenomenon that, in these circumstances, the particle fraction has a value of -1 and, because the external porosity is defined as the difference between unity and the particle fraction, its value is always 2, for a filled empty conduit. This counter intuitive phenomenon can be rationalized by a comparison to the phenomenon embedded in the permeability equation, wherein the fluid velocity has a negative sign, in the differential form of that equation (Navier-Stokes), and represents the physical reality that liquids flow downhill in the direction of the pressure gradient, i.e., the flow moves from high pressure to low pressure coordinates, which means that the variables of resultant pressure, $P = (\rho_f g L)$, and consequential velocity, $\mu_s = \pi D^2 L/(4q)$, in the mathematical milieu of the Navier-Stokes equation, move in opposite directions.

References.

[1] Poiseuille, J. L. (1841). "Recherches expérimentales sur le mouvement des liquides dans les tubes de très-petits diamètres." Comptes Rendus, Académie des Sciences, Paris 12, 112 (in French).

[2] H. Darcy, *Les Fontaines Publiques de la Ville de Dijon*, Victor Dalmont, Paris, France, 1856.

[3]J.L.M. Poiseuille, Memoires des Savants Etrangers, Vol. IX pp. 435-544, (1846);. Brillouin, Marcel (1930). "Jean Leonard Marie Poiseuille". *Journal of Rheology*. **1**: 345. doi:10.1122/1.2116329

[4H. M. Quinn, “Reconciliation of packed column permeability data, column permeability as a function of particle porosity,” *Journal of Materials*, vol. 2014, Article ID 636507, 22 pages, 2014.

[5] J. M. Coulson; University of London, Ph.D. thesis, “The Streamline Flow of Liquids through beds comprised of Spherical particles” 1935.

[6] A. O. Oman and K. M. Watson, “Pressure drops in granular beds,” *National Petroleum News*, vol. 36, pp. R795–R802, 1944.

[7] M. Leva and M. Grummer, “Pressure drop through packed tubes, part I, a general correlation,” vol. 43, pp. 549–554, 1947.

[8] F. A. L. Dullien, *Porous Media, Fluid Transport and Pore Structure*, Acedemic Press, 2nd edition, 1979.

[9]S. W. Churchill, *Viscous Flows: The Practical Use of Theory*, Butterworks, 1988.

[10] S. P. Burke and W. B. Plummer, “Gas flow through packed columns,” *Industrial and Engineering Chemistry*, vol. 20, pp. 1196–1200, 1923

[11] J. C. Giddings, Dynamics of Chromatography, Part I, Principles and Theory, Marcel Dekker, Inc. New York, (1965

[12] T. Farkas, G. Zhong, G. Guiochon, Journal of Chromatography A, 849, (1999) 35-43

[13] M. Rhodes, Introduction to Particle technology, John Wiley & Sons, Inc., p. 83 (1998).

[14] G. O. Brown., 1999-2006, Henry Darcy and His Law, www.biosystems.okstate.edu/Darcy.

[15]I. Halasz, M. Naefe, Analytical Chemistry, 44 (1972) 76

[16] F. E. Blake, “The resistance of packing to fluid flow,” *Transaction of American Institute of Chemical Engineers*, vol. 14, pp. 415–421, 1922.

[17] J. Kozeny, “Uber kapillare Leitung des wassers in Böden,” *Sitzungsberichte der Kaiserlichen Akademie der Wissenschaften*, vol. 136, pp. 271–306, 1927.

[18] Carman, P.C., “Fluid flow through granular beds,” Transactions of the Institution of Chemical Engineers, vol. 15, pp. 155–166, 1937.

[19] Bird, R. B., Stewart, W. E., Lightfoot, E. N. Transport Phenomena, John Wiley & Sons, Inc., p. 190,

[20] H. M. Quinn, Reconciliation of Packed Column Permeability Data-Part 1. The Teaching Of Giddings Revisited, Special Topics & Reviews in Porous Media-An International Journal 1 (1), (2010) 79-86

[21] Halasz, R. Endele, K. Unger, Journal of Chromatography, 99 (1974) 377-393

[22] G. Guiochon, Chromatographic Review, 8 (1966)

[23]A. E. Scheidegger, *The Physics of Flow Through Porous Media*, MacMillan Company, New York, NY, USA, 1957.

[24] J. Kozeny, "Ueber kapillare Leitung des Wassers im Boden." Sitzungsber Akad. Wiss., Wien, 136(2a): 271-306, 1927

[25] J. C. Giddings, Unified Separation Science, John Wiley & Sons (1991)

[26] Halasz, R. Endele, K. Unger, Journal of Chromatography, 99 (1974) 377-393

[27] U. Neue, HPLC Columns-Theory, Technology and Practice, Wiley-VCH (1997)

[28] P.C. Carman, Trans. Instn. Chem. Engrs. Vol. 15, (1937) 155-166

[29] J. M. Godinho, A. E. Reising, U. Tallarek, J. W. Jorgenson; Implementation of high slurry concentration and sonication to pack high-efficiency, meter-long capillary ultrahigh pressure liquid chromatography columns: Journal of Chromatography A, 1462 (2016) 165-169

[30]L. R. Snyder, J.J. Kirkland, Introduction to Modern Liquid Chromatography, 2nd Edition, John Wiley & Sons, Inc. p. 37 (1979)

[31]G. Guiochon, S. G. Shirazi, A. M. Katti, Fundamentals of Preparative and Nonlinear Chromatography, Academic Press, Boston, Ma, (1994).

[32]S. Ergun and A. A. Orning, “Fluid flow through randomly packed columns and fluidized beds,” *Industrial & Engineering Chemistry*, vol. 4, no. 6, pp. 1179–1184, 1949.

[33] Ergun, Chem. Eng. Progr. 48 (1952) 89-94.

[34]I. F. Macdonald, M. S. El-Sayed, K. Mow, and F. A. L. Dullien *Industrial & Engineering Chemistry Fundamentals* **1979** *18* (3), 199-208 DOI: 10.1021/i160071a001

[35] J. Happel and H. Brenner, *Low Reynolds Number Hydrodynamics*, Prentice-Hall, 1965

[36] Reynolds O. 1883. An experimental investigation of the circumstances which determine whether the motion of water in parallel channels shall be direct or sinuous and of the law of resistance in parallel channels.Philos.Trans.R.Soc.174:935–82

[37]J. Nikuradze, NASA TT F-10, 359, Laws of Turbulent Flow in Smooth Pipes. Translated from “Gesetzmassigkeiten der turbulenten Stromung in glatten Rohren” VDI (Verein Deutsher Ingenieure)-Forschungsheft 356.

[38] J. Nikuradze, NACA TM 1292, Laws of Flow in Rough Pipes, July/August 1933. Translation of “Stromungsgesetze in rauhen Rohren.” VDI-Forschungsheft 361. Beilage zu “ Forschung auf dem Gebiete des Ingenieurwesens” Ausgabe B Band 4, July/August 1933.

[39] L. Prandtl, in Verhandlungen des dritten internationalen Mathematiker-Kongresses in Heidelberg 1904, A. Krazer, ed., Teubner, Leipzig, Germany (1905), p. 484. English trans. in Early Developments of Modern Aerodynamics, J. A. K. Ackroyd, B. P. Axcell, A. I. Ruban, eds., Butterworth-Heinemann, Oxford, UK (2001), p. 77.

[40]Moody, L. F. (1944). "Friction factors for pipe flow." Trans. ASME, 66:671-678.

[41]Studies and Research on Friction, Friction Factor and Affecting Factors : A Review

Sunil J. Kulkarni *, Ajaygiri K. Goswami; Chemical Engineering Department,, Datta Meghe College of Engineering, Airoli, Navi Mumbai, Maharashtra, India

[42]Technical Note: Friction Factor Diagrams for Pipe Flow; Jim McGovern Department of Mechanical Engineering and Dublin Energy Lab Dublin Institute of Technology, Bolton Street Dublin 1, Ireland

[43] B. J. Mckeon, C. J. Swanson, M. V. Zagarola, R. J. Donnelly and A. J. Smits. Friction factors for smooth pipe flow; J. Fluid Mech. (2004), vol. 511, pp. 41-44. Cambridge University Press; DO1; 10.1017/S0022112004009796.

[44] Unified fluid flow model for pressure transient analysis in naturally fractured media; Petro Babak[1] and Jalel Azaiez; Journal of Physics A: Mathematical and Theoretical, Volume 48, Number 17

[45]Quinn, H. M. Quinn’s Law of Fluid Dynamics Pressure-driven Fluid Flow Through Closed Conduits, *Fluid Mechanics*. Vol. 5, No. 2, 2019, pp. 39-71. doi: 10.11648/j.fm.20190502.12

[46] Jan H. van Lopik1 · Roy Snoeijers1 · Teun C. G. W. van Dooren1 · Amir Raoof1 · Ruud J. Schotting; Transp Porous Med (2017) 120:37–66 DOI 10.1007/s11242-017-0903-3

[47] Forchheimer, P.: Wasserbewegung durch boden. Zeit. Ver. Deutsch. Ing **45**, 1781–1788 (1901)

Appendix

Glossary of Terms

QFFM Reference guide for Fluid Dynamics

Ref: Quinn's Law of Fluid Dynamics Pressure-driven Fluid Flow Through Closed Conduits. *Fluid Mechanics.*

Vol. 5, No. 2, 2019, pp. 39-71. doi: 10.11648/j.fm.20190502.12

#	Symbol	Unit cgs	Ref.	Formula	Description
				Particle	**Independent variable**
1	$\mathbf{d_{pm}}$	cm	Sec 2.2.1	N/A	Particle nominal diameter
2	$\mathbf{\Omega_p}$	none	Sec 2.2.1	N/A	Particle sphericity
3	$\mathbf{S_{pv}}$	cm^3g^{-1}	Sec 2.2.1	N/A	Particle specific pore volume
4	$\mathbf{\rho_{sk}}$	gcm^{-3}	Sec 2.2.1	N/A	Particle skeletal density
5	$\mathbf{m_{dp}}$	g	Sec 2.2.1	N/A	Mass of the particle
					Dependent variable
6	$\mathbf{d_p}$	cm	Eq (1)	$\mathbf{\Omega_p d_{pm}}$	Spherical particle diameter equivalent
7	$\mathbf{SA_p}$	cm^2	Eq (2)	$\mathbf{\pi d_p^2}$	Surface area of spherical particle equivalent
8	$\mathbf{CSA_p}$	cm^2	Eq (3)	$\mathbf{\pi d_p^2/4}$	Cross-sectional area of spherical particle equivalent
9	$\mathbf{V_{dp}}$	cm^3	Eq (4)	$\mathbf{\pi d_p^3/6}$	Volume of spherical particle equivalent
10	$\mathbf{\rho_{part}}$	g	Eq (5)	$\mathbf{m_{dp}/V_{dp}}$	Particle apparent density
11	$\mathbf{\varepsilon_p}$	none	Eq (6)	$\mathbf{S_{pv}\rho_{part}}$	Particle porosity
				Conduit	**Independent variable**
12	**D**	cm	Sec 2.2.2	N/A	Conduit diameter
13	**L**	cm	Sec 2.2.2	N/A	Conduit length
14	**k**	cm	Sec 2.2.2	N/A	Conduit wall roughness dimension
15	$\mathbf{n_p}$	none	Sec 2.2.2	N/A	Number of particle equivalents in conduit under study
					Dependent variable
16	$\mathbf{V_{ec}}$	cm^3	Eq (7)	$\mathbf{\pi D^2 L/4}$	Empty conduit volume expressed in terms of conduit diameter and length
17	$\mathbf{V_{part}}$	cm^3	Eq (8)	$\mathbf{n_p V_{dp}}$	Conduit volume occupied by all the particles
18	$\mathbf{n_{pq}}$	none	Eq (9)	$\mathbf{3D^2L/(2d_p^3)}$	Dimensionless empty conduit volume (number of spherical particle equivalents)
19	$\mathbf{\gamma}$	none	Eq (10)	$\mathbf{n_{pq}D/L}$	Conduit architectural coefficient
				Q porosity Functions	**Independent variable**
20	$\mathbf{V_e}$	cm^3	Sec 2.2.2	N/A	Conduit volume *external* to the particle fraction
21	$\mathbf{V_i}$	cm^3	Sec 2.2.2	N/A	Conduit volume *internal* to the particle fraction
22	$\mathbf{V_{sk}}$	cm^3	Sec 2.2.2	N/A	Conduit volume occupied by the cumulative skeletons of all the particles

23	V_t	cm^3	Sec 2.2.2	N/A	Conduit volume excluding the volume occupied by the particle skeletons
					Dependent variable
24	$(1-\varepsilon_0)$	none	Eq (11)	n_p/n_{pq}	Conduit particle volume fraction
25	ε_0	none	Eq (12)	$(1-n_p/n_{pq})$	Conduit external porosity; volume fraction external to particles
26	ε_i	none	Eq (13)	$\varepsilon_p(1-\varepsilon_0)$	Conduit internal porosity; volume fraction internal to particles (porous)
27	ε_t	none	Eq (14)	$1-(1-\varepsilon_p)n_p/n_{pq}$	Conduit total porosity; sum of external and internal volume fraction (porous)
28	ε_{sk}	none	Eq (15)	$n_p(1-\varepsilon_p)/n_{pq}$	Conduit particle skeletal fraction; volume fraction occupied by skeleton of particle fracti
29	$n_p\pi d_p^3/6$	none	Eq (16)	$V_{ec}abs(1-\varepsilon_0)$	Reconciliation between solids and porosity in packed conduit
				Governing Principle	**Continuity Laws**
32	**Unity**	none	Eq (17)	$\varepsilon_0+\varepsilon_i+\varepsilon_{sk}$	Conservation Law (porous particles)
33	**Unity**	none	Eq (18)	$\varepsilon_t+\varepsilon_{sk}$	Conservation Law
34	ρ_{pack}	gcm^{-1}	Eq (19)	M_p/V_{ec}	Conduit packing density
35	ε_0	none	Eq (20)	$1-\rho_{pack}(S_{pv}-1/\rho_{sk})$	Conduit external porosity (mass of particles based)
36	ε_0	none	Eq (21)	$1-(2n_pd_p^3/(3D^2L))$	Conduit external porosity (number of particles based)
37	ε_p	none	Eq (22)	$(\varepsilon_t-\varepsilon_o)/(1-\varepsilon_0)$	Particle porosity (measurements made *inside* packed conduit)
38	$S_{pv}\rho_{part}$	none	Eq (23)	$(\varepsilon_t-\varepsilon_o)/(1-\varepsilon_0)$	Particle porosity (measurements made *outside* packed conduit) i.e. *independent*
39				**Hypothetical Q Channel**	**Dimensional parameters (scale factor)**
40	d_c	cm	Eq (24)	$d_p/(abs(1-\varepsilon_0))$	HQC diameter under study
41	v_c	cm^3	Eq (25)	$\pi n_{pq}d_p^3\varepsilon_t/6$	HQC volume under study
42	a_c	cm^2	Eq (26)	$\pi n_{pq}^2d_p^2/(4n_p^2)$	HQC cross sectional area
43	l_c	cm	Eq (27)	$2n_p^2d_p\varepsilon_t/(3n_{pq})$	HQC length under study
					Uniform Circular motion
44	ΔP	$gcm^{-1}sec^{-2}$	Eq (28)	P_1-P_0	Conduit Differential pressure
45	ω	$radsec^{-1}$	Eq (29)	$d\Phi/dt$	Angular velocity
46	Φ	radians	Eq (30)	$(\omega t+\alpha)$	Phase of the motion
47	x	cm	Eq (31)	$acos(\omega t+\alpha)$	x coordinate displacement
				QFFM	**Dimensionless manifestation**
48	P_Q	none	Eq (32)	$(k_1+\lambda Q_N/\phi_h)$	Viscous normalized friction factor
49	P_K	none	Eq (33)	P_Q/Q_N	Kinetic normalized friction factor
50	Θ	none	Eq (34)	Q_N/P_Q	Dimensionless permeability
51	Θ	none	Eq (35)	$1/(k_1/Q_N+\lambda/\phi_h)$	Dimensionless permeability
				QFFM	**Reference parameters**
52	π	none	N/A	22/7	Universal constant
53	ϕ_h	none	Eq (36)	$2\pi r_h=8\pi$	Drag normalized hydraulic channel circumference
54	k_2		Eq (37)	$1/\phi_h=1/(8\pi)$	Fluid kinetic control element normalization coefficient
55	r_h	none	Eq (38)	$SA_p/CSA_p=4$	Normalization coefficient of fluid drag
56	k_1	none	Eq (39)	$4/3\pi r_h^2=67$	Fluid viscous control element normalization coefficient

				Fluid Dynamics	Parameters
57	P_Q	none	Eq (40)	$64\pi/3 + \lambda Q_N/8\pi$	Viscous normalized friction factor
58	δ	none	Eq (41)	$1/\varepsilon_0^3$	Conduit porosity normalization coefficient
59	τ	none	Eq (42)	$\delta\gamma$	Conduit tortuosity normalization coefficient
60	Q_N	none	Eq (43)	δR_{em}	Fluid current
61	λ	none	Eq (44)	$(1+W_N)$	Fluid current wall normalization coefficient
62	P_Q	none	Eq (45)	$64\pi/3 +\delta\lambda R_{em}/(2\pi r_h)$	Viscous normalized friction factor
63	P_Q	none	Eq (46)	$64\pi/3 +\delta(1+W_N)R_{em}/(2\pi r_h)$	Viscous normalized friction factor
64	W_N	none	Eq (47)	$W_1 + W_{2R}$	Net wall effect
65	ω_0	none	Eq (48)	$1/\phi_h$	Dimensionless fluid resistance
66	β_0	none	Eq (49)	$k_1/(k_2Q_N+k_1)$	Viscous boundary layer (λ =1)
67	W_1	none	Eq (50)	$\beta_0^{(1/3)}/\tau$	Primary wall effect
68	k_{dc}	none	Eq (51)	k/d_c	Relative wall roughness coefficient
69	W_2	none	Eq (52)	$30k_{dc}^{(1/3)}$	Secondary wall effect
70	W_{2R}	none	Eq (53)	W_2-$W_1^{(1.2)}$	Residual secondary wall effect ($W_{2R} \geq 0$)
71	R_{em}	none	Eq (54)	$4qd_c\rho_f/(\pi\eta D^2)$	Modified Reynolds number
72	n_k	$gcm^{-2}sec^{-2}$	Eq (55)	$\delta\mu_s^2\rho_f/d_c$	the *kinetic* hydraulic force exerted *per unit element of fluid control volume*
73	μ_s	$cmsec^{-1}$	Eq (56)	$4q/(\pi D^2)$	Average fluid superficial linear velocity (fluid flux).
74	n_v	$gcm^{-2}sec^{-2}$	Eq (57)	$\delta\mu_s\eta/d_c^2$	the *viscous* hydraulic force exerted *per unit element of fluid control volume*
75	BLT	cm	Eq (58)	$\beta d_c/(2\tau)$	Boundary layer thickness
76	P_Q	none	Eq (59)	$4\pi r_h^2/3 + \delta\lambda n_k/(2\pi r_h n_v)$	Viscous friction factor
77	$\Delta P/(r_h n_v L)$	none	Eq (60)	P_Q	Drag normalized viscous friction factor
78	$\Delta P/(r_h n_v L)$	none	Eq (61)	$4\pi r_h^2/3 + \delta\lambda n_k/(2\pi r_h n_v)$	Drag normalized viscous friction factor
79	$\Delta P/(r_h L)$	$gcm^{-2}sec^{-2}$	Eq (62)	$4\pi r_h^2 n_v/3 + \delta\lambda n_k/(2\pi r_h)$	Drag normalized pressure gradient
80	$\Delta P/L$	$gcm^{-2}sec^{-2}$	Eq (63)	$4\pi r_h^3 n_v/3 + \delta\lambda n_k/2\pi$	Total pressure gradient
81	$\Delta P/L$	$gcm^{-2}sec^{-2}$	Eq (64)	$4\pi r_h^3\delta\mu_s\eta/(3d_c^2) + \delta^2\lambda\mu_s^2\rho_f/dc$	QFFM practitioner's empirical equation
82	$\Delta P/L$	$gcm^{-2}sec^{-2}$	Eq (65)	$4\pi r_h^3 n_v/3$	Viscous pressure gradient
83	C_Q	none	Eq (66)	λQ_N	Wall normalized instantaneous fluid current
84	β	none	Eq (67)	$k_1/(k_2C_Q+k_1)$	Instantaneous boundary layer
85	P_Q	none	Eq (68)	$64\pi/3 + C_Q/(8\pi)$	Quinn's Law
86	$\Delta P/L$	$gcm^{-2}sec^{-2}$	Eq (69)	$1024\delta q\eta/(3D^2d_c^2) + 8\delta^2\lambda q^2\rho_f/(\pi^3D^4d_c)$	QFFM expanded equation
87	$\Delta P/L$	$gcm^{-2}sec^{-2}$	Eq (70)	$128q\eta/(3D^4) + \lambda q^2\rho_f/(248D^5)$	QFFM balanced equation for empty conduit
				QFFM	Dimensional manifestation
88	q	cm^3sec-1	Sec 2.3.3	dv/dt	Fluid volumetric flow rate
89	η	$gcm^{-1}sec^{-1}$	Sec 2.3.3	N/A	Fluid absolute viscosity
90	ρ_f	gcm^{-3}	Sec 2.3.3	N/A	Fluid density

91	**ν**	cm^2sec^{-1}		**η/ρ_f**	Fluid kinematic viscosity
92	**λ_{bc}**	none		**$\pi^3D^4d_c(\Delta P\text{-}bq)/(8\delta^2\rho_fLq^2)$**	Back-calculated wall normalization coefficient
93	**QFFM**	none	Eq (71)	**$aq^2+bq+c = 0$**	Quadratic manifestation
94	**c**	$gcm^{-1}sec^{-2}$	Eq (72)	**$-\Delta P$**	constant
95	**ΔP**	$gcm^{-1}sec^{-2}$	Eq (73)	**aq^2+bq**	Calculated differential pressure drop
96	**q_{bc}**	m^3sec^{-1}	Eq (74)	**$-b\pm\sqrt{(b^2-4ac)}/(2a)$**	Back-calculated flow rate from measured pressure differential
97	**a**	gcm^{-7}	Eq (75)	**$8\delta^2\lambda\rho_fL/(\pi^3D^4d_c)$**	Quadratic term coefficient (flow rate based)
98	**b**	$gcm^{-4}sec^{-1}$	Eq (76)	**$1024\delta\eta L/(3D^2d_c^2)$**	Linear term coefficient (flow rate based)
99	**$\Delta P/L$**	$gcm^{-2}sec^{-2}$	Eq (77)	**$1024(1-\varepsilon_0)^2q\eta/(3D^2d_c^2) + 8(1-\varepsilon_0)\lambda q^2\rho_f/(\pi^3D^4\varepsilon_0^6d_c)$**	Total pressure gradient
100	**$\Delta P/L$**	$gcm^{-2}sec^{-2}$	Eq (78)	**$256\pi(1-\varepsilon_0)^2\mu_s\eta/(3\varepsilon_0^3d_p^2) + (1-\varepsilon_0)\lambda\rho_f\mu_s^2/(2\pi\varepsilon_0^6d_p)$**	Q modified Ergun equation
101	**$\Delta P/L$**	$gcm^{-2}sec^{-2}$	Eq (79)	**$A(1-\varepsilon_0)^2\mu_s\eta/(\varepsilon_0^3d_p^2) + B(1-\varepsilon_0)\rho_f\mu_s^2/(\varepsilon_0^3d_p)$**	Q modified Ergun equation
102	**A**	none	Sec. 2.34	**$256\pi/3$**	Q modified Ergun (viscous) constant
103	**B**	none	Sec. 2.34	**$\lambda/(2\pi e_0^3)$**	Q modified Ergun (kinetic) constant
104	**τ_w**	$gcm^{-1}sec^{-2}$	Eq (82)	**$\Delta PD/(4L)$**	Wall shear stress
				Harmonic Oscillator	**Parameters**
					Damping Coefficients
105	**v**	$cmsec^{-1}$	Eq (80)	**$v_x+v_y+v_z$**	Instantaneous fluid velocity
106	**t_0**	sec	Eq (81)	**$(\pi D^2L\varepsilon_t)/4q$**	Time to displace one (packed) conduit volume
107	**μ_f**	$cmsec^{-1}$	Eq (83)	**$(\tau_w/\rho_f)^{(1/2)}$**	Fluid frictional velocity
					SHM dimensional parameter equivalents
108	**t**	sec	Sec 3	**Q_N**	Elapsed time
109	**α**	radians	Sec 3	**$k_1(2\pi/360)$**	Epoch of the motion
110	**ω_0**	$radsec^{-1}$	Sec 3	**k_2**	Reference angular velocity (when there is no net wall effect; $W_N = 0$; $\lambda = 1$)
111	**ω**	$radsec^{-1}$	Sec 3	**λ/ϕ_h**	Instantaneous angular velocity
112	**Φ**	radians	Sec 3	**P_Q**	Phase of the motion
113	**T**	sec	Eq (84)	**$2\pi/\omega$**	Period of the motion
114	**ϕ**	$radsec^{-1}$	Eq (85)	**1/T**	Frequency of the motion
115	**M_0**	cm	Eq (86)	**$d_c/2$**	Maximum amplitude displacement (scale factor)
116	**M**	cm	Eq (87)	**$M_0exp^{(-\omega t o)}$**	Instantaneous amplitude displacement
					Dimensional x-coordinate
117	**x**	cm	Eq (88)	**$McosP_Q$**	Instantaneous displacement in x direction
118	**V_x**	$cmsec^{-1}$	Eq (89)	**$-M\lambda/\phi_hsinP_Q$**	Instantaneous velocity in x direction
119	**f_x**	$cmsec^{-2}$	Eq (90)	**$-M(\lambda/\phi_h)^2cosP_Q$**	Instantaneous acceleration in x direction
					Dimensional y-coordinate
120	**y**	cm	Eq (91)	**$MsinP_Q$**	Instantaneous displacement in y direction
121	**V_y**	$cmsec^{-1}$	Eq (92)	**$M(\lambda/\phi_h)cosP_Q$**	Instantaneous velocity in y direction

122	$\mathbf{f_y}$	$cmsec^{-2}$	Eq (93)	$\mathbf{-M(\lambda/\phi_h)^2 sinP_Q}$	Instantaneous acceleration in y direction
					Dimensional z-coordinate
123	**z**	cm	Eq (94)	$\mathbf{Mcos(\pi/4\text{-}P_Q)}$	Instantaneous displacement in y direction
124	$\mathbf{V_z}$	$cmsec^{-1}$	Eq (95)	$\mathbf{-M(\lambda/\phi_h)sin(\pi/4\text{-}P_Q)}$	Instantaneous velocity in y direction
125	$\mathbf{f_z}$	$cmsec^{-2}$	Eq (96)	$\mathbf{-M(\lambda/\phi_h)^2 cos(\pi/4\text{-}P_Q)}$	Instantaneous acceleration in y direction
					Dimensionless x-coordinate
126	**x***	none	Eq (97)	$\mathbf{(M_0\text{-}x)/(2M_0)}$	Unit cell displacement in x direction
127	$\mathbf{V_x}$*	none	Eq (98)	$\mathbf{V_x/\mu_f}$	Unit cell velocity in x direction
					Dimensionless y-coordinate
128	**y***	none	Eq (99)	$\mathbf{(M_0\text{-}y)/(2M_0)}$	Unit cell displacement in y direction
129	$\mathbf{V_y}$*	none	Eq (100)	$\mathbf{V_y/\mu_f}$	Unit cell velocity in y direction
					Dimensionless z-coordinate
130	**z***	none	Eq (101)	$\mathbf{(M_0\text{-}z)/(2M_0)}$	Unit cell displacement in z direction
131	$\mathbf{V_z}$*	none	Eq (102)	$\mathbf{V_z/\mu_f}$	Unit cell velocity in y direction